University of BRISTOL

Department Of Physics

FINAL YEAR PROJECT, DISSERTATION OR PHYSICS EDUCATION REPORT

NAME:	Luka Milic
DEGREE COURSE:	Mathematics and Physics (MSci)
PROJECT TITLE:	Entanglement of photons pairs generated in silicon ring resonators
YEAR OF SUBMISSION:	2015
SUPERVISOR:	Damien Bonneau, Josh Silverstone and Mark Thompson
NUMBER OF WORDS:	2059 (exclude appendices, references, captions and abstract)

Entanglement of photons pairs generated in silicon ring resonators

Luka Milic

April 13, 2015

Abstract

Do the abstract last.

Acknowledgements

Thank you Damien and Josh for your invaluable help throughout my project. Lizzy for working with me in the lab. Imad for your help and encouragement. Mark for giving me the opportunity and supervision. Raf for your help and Phil for supplying sarcasm.

Contents

1 Introduction

The endeavour to build a quantum computer holds the promise of solving computational problems which are currently intractable on classical computers. A particularly promising paradigm for this is the linear optical quantum computer (LOQC) model which in theory allows for scalable universal quantum computation. Work on LOQC can be done using bulk optics components but this quickly becomes impractical when the experiments need to be scaled up to more qubits. Integrated photonics is a solution to this problem and allows for experiments a much higher component density, an essential ingredient to scalable quantum computing. General optical circuits can be implemented on such chips, popular materials are silicon-on-insulator (SOI) , lithium niobate and glass materials. Here we focus on SOI chips as they have many promising properties for the implementation of complex quantum optical circuits.

A key requirement for the full implementation of LOQC is a scalable, bright, deterministic and indistinguishable single photon source. Single photon sources in the SOI platform are typically made from the waveguide itself and use the spontaneous four-wave mixing which occurs in silicon due to the third order non-linearity to create a single photon pair. This report aims to develop a method of measuring the indistinguishably of the produced photons with a classical technique, exploiting stimulated four-wave mixing. This method collects a joint spectrum which is an estimation of the spectral shape of the two photons produced by the source. For a full description the Joint Spectral Amplitude JSA is the desired quantity, this is a full description of the wavefunction of the single photons emitted by the silicon ring resonators. However it is only within the scope of this work to measure the Joint Spectral Intensity, which is the absolute value squared the JSI. This gives an estimate of the JSA and allows to to upper bound the purity of the source.

The mission is therefore to develop a methodology to reconstruct these wavefunctions and hence engineer indistinguishable (high purity) single photon sources. In this work we performed such measurements on three SOI chips. The experimental work started with an initial proof of concept that one can collect joint spectrum data in the way desired. This was done on a chip supplied by Marc Sorel from Glassgow University. Then due to the fragility of these chip at high powers the experiment progressed to a chip manufactured by Toshiba. Finally in order to investigate a promising new material, amorphous silicon chip was used for experiments.

In parallel techniques of analysing the output data are developed. Filtering techniques which remove noise are developed in order to make the data usable. A general framework is set out which aims to quantify the certainty in the measurements.

Finally we conclude that there is still much to be done in this area, proposing an outline for how to carry out effective measurements in the future.

2 Detailed Background and Theory

2.1 From Feynman to the linear optical quantum computer

It was Richard Feynman in 1982 who first imagined it might be possible to efficiently simulate quantum systems with other quantum systems and hence end up doing computations that no classical computer could do in a reasonable (polynomial) time. Since then the theory has come a long way and there are many diverse research efforts trying to realise his idea. The work in this report is motivated by a particular paradigm called the linear optical quantum computer LOQC or often called the KLM protocol [1], this requires only standard optical elements to be able to fully simulate a quantum computer. This is inline with the five requirements set out by DiVincenzo in 1998 [2] for a full quantum computer.

- A scalable physical system with well characterized qubits
- The ability to initialize the state of the qubits to a simple fiducial state, such as $|000...\rangle$
- Long relevant decoherence times, much longer than the gate operation time
- A universal set of quantum gates
- A qubit-specific measurement capability

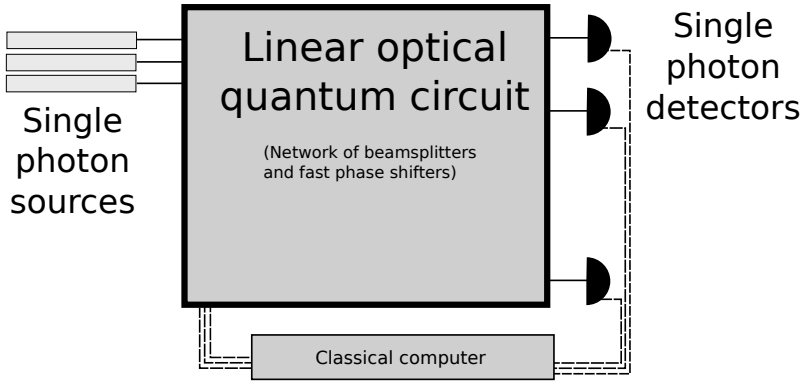

Figure 2.1: A conceptual outline of the architecture of a LOQC, single photon sources supply the qubits which are fed into reconfigurable circuits which are altered depending on the pattern of photons detected at the detectors.

We focus in on the first criteria from DiVencenzo [3], "A scalable system with well characterized qubits", which in the context of figure 2.1 refers to the single photon sources. This criteria tell us that our photons must have no degrees of freedom apart from the one which allows the photons to act as qubits. A particular way in which the photons might be different is in their spectral and phase distribution. This is described by their Joint Spectral Amplitude (JSA)

2.2 From bulk optics to integrated silicon photonics

Quantum optics experiments were first conducted in bulk optics [4] and since then they have allowed for the development of a large body of physics. Such experiments have certain basic elements in

common such as beam splitters, filters, polarisation controllers, phase shifters, etc. With these elements occupying a fair amount of space in a lab there is a practical size limit on what can be done, hence there has been a recent push into compressing such optical experiments onto a single chip. Each of the optical elements described previously can be implemented onto such chips. The free space propagation of light is replaced by waveguides etched onto materials such as silicon, lithium niobate or glass. Beam splitters and couplers are implemented by running two waveguides close enough to each other so that light can couple between them via their evanescent fields. Filters are implemented as ring resonators which are circular cavaties with which only certain wavelengths of light will resonate and hence be filtered. Phase shifts can be induced by heating small portions of the chip with an electrical probe.

Here we focus in on a particular element, the ring resonator on silicon photonic devices. Silicon is an attractive material primarily due to the already established microchip industry which can produce highly precise structures at the nanoscale on the back of decades of demand for faster and smaller computing devices. Furthermore silicon has a high $\chi^{(3)}$ non-linearity enabling frequency conversion and hence the implementation of a single photon source.

2.3 Four wave mixing in silicon waveguides

$$\nabla^2\mathbf{E} - \frac{n^2}{c^2}\frac{\partial^2}{\partial t^2}\mathbf{E} = \frac{1}{\varepsilon_0 c^2}\frac{\partial^2}{\partial t^2}\mathbf{P}^{NL} \tag{2.1}$$

2.4 Ring Resonators

Ring resonators are used enhance the generation of photons in the waveguide in a few key ways. However to understand their behaviour to first order no quantum mechanics is needed. Here are the 3 governing equations:

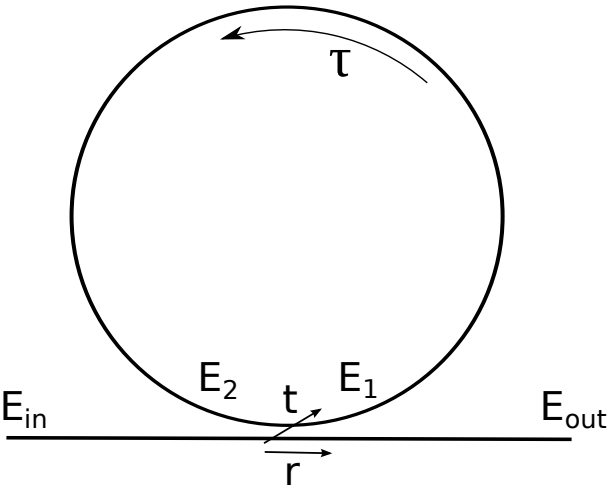

Figure 2.2: A simple but powerful model of a ring resonator. E_{in} represents the input electrical field and E_{out} is the field after interaction with the ring. E_1 is the field at the start of the ring and E_2 is this field with some loss due to propagation through the ring waveguide. We assume that the distance between E_{out} and E_{in} is much smaller than E_1 and E_2.

$$\left|\frac{E_{out}}{E_0}\right|^2 = \frac{r^2 - 2r\tau\cos(\theta) + \tau^2}{1 + r^2\tau^2 - 2r\tau cos(\theta)} \tag{2.2}$$

$$\left|\frac{E_1}{E_0}\right|^2 = \frac{t^2}{1 + r^2\tau^2 - 2r\tau cos(\theta)} \tag{2.3}$$

$$\left|\frac{E_2}{E_0}\right|^2 = \tau^2 \left|\frac{E_1}{E_0}\right|^2 \tag{2.4}$$

SPLIT RESONANCES

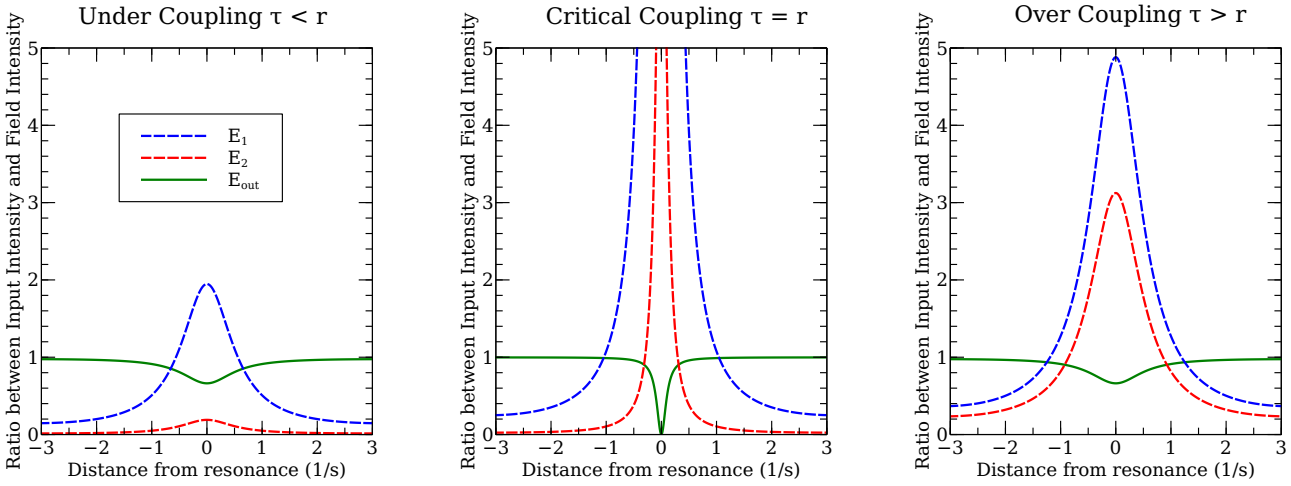

Figure 2.3: Notice how similar under and over coupling are to each other

2.5 Bistability

It can be experimentally observed that injecting power into a ring resonator will cause changes in the spectral position and shape of the resonance. Typically in silicon ring resonators the more power in the ring the more the resonance position is red-shifted by the thermo-optic effect [5]. A counter acting effect is carrier generation induced by two-photon absorption [6] which causes a blue-shift in the resonance position. This carrier generation process is much faster than the thermo-optic process so it more relevant to lasers with low repetition rates.

The bi-stability effect is observed by changing the power injected into the ring resonator at a fixed wavelength. By steadily increasing the power of a monochromatic light source injected into the ring at a wavelength slightly higher than the resonance position λ_r of the ring, λ_r is increased (thermal effects dominate as the laser is a continuous wave and not pulsed). The shift in λ_r accelerates as more light is coupled into the ring and transmission falls as more light is coupled into the ring. The system is now in a different and stable state (assuming the injected light is not discontinued). With a low intensity probe it is now possible to map out the new position and shape of the resonance.

By doing the reverse experiment with the input power decreasing a similar phenomena is observed, however the sudden accelerating changing in resonance position is seen for a different power due to the ring coming from a different stable state.

Some knowledge of this effect is vital when planning experiments using high and variable powers, as one must take into account which state the ring is in. Further when automating equipment it may be vital to integrate knowledge of this into any scanning procedures.

2.6 Characterisation of quantum processes with classical techniques

Marco [7]

2.7 Schmidt Rank and Purity

2.8 Self phase modulation

3 Method

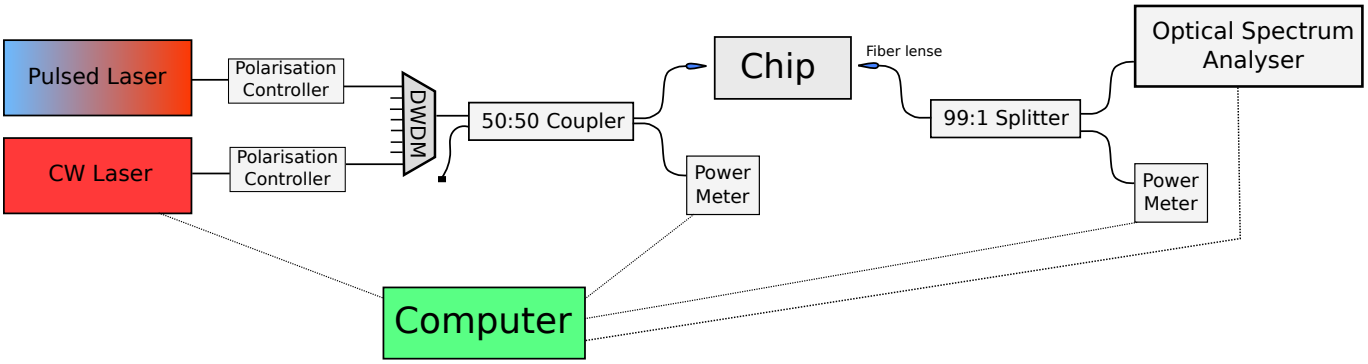

Figure 3.1: Glassgow test structure chip

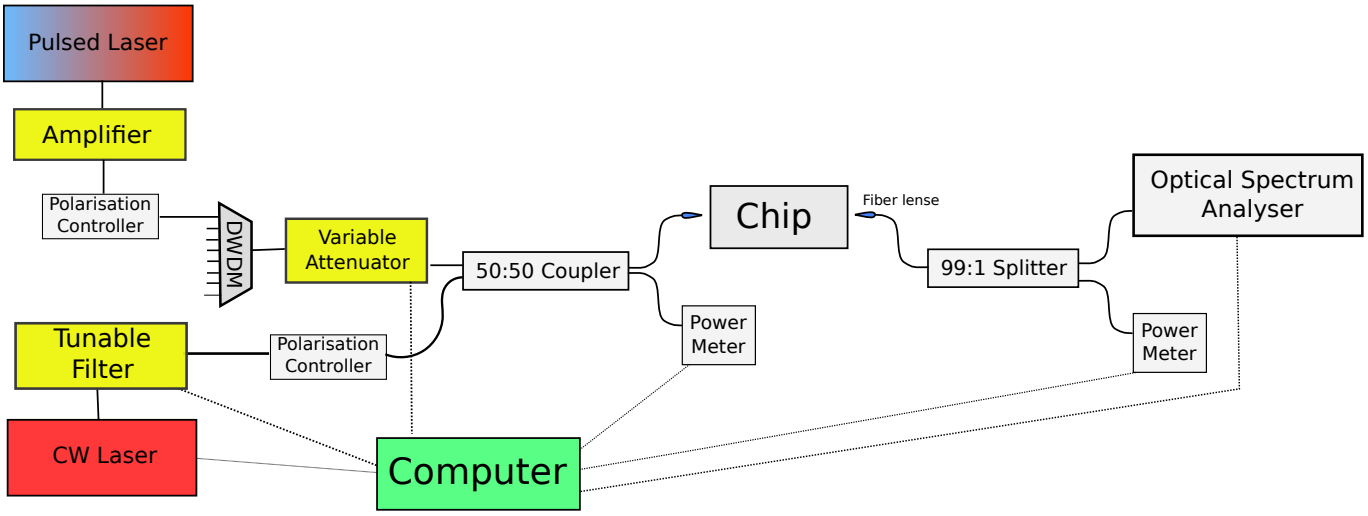

Figure 3.2: Glassgow test structure chip

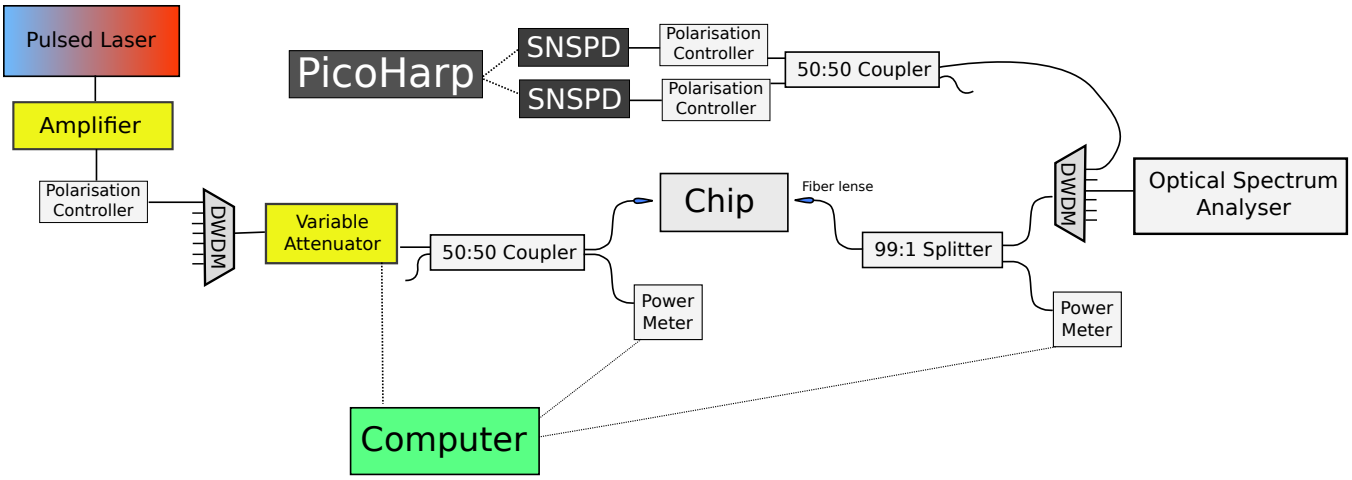

Figure 3.3: Glassgow test structure chip

3.1 Silicon Chips

3.1.1 Glassgow

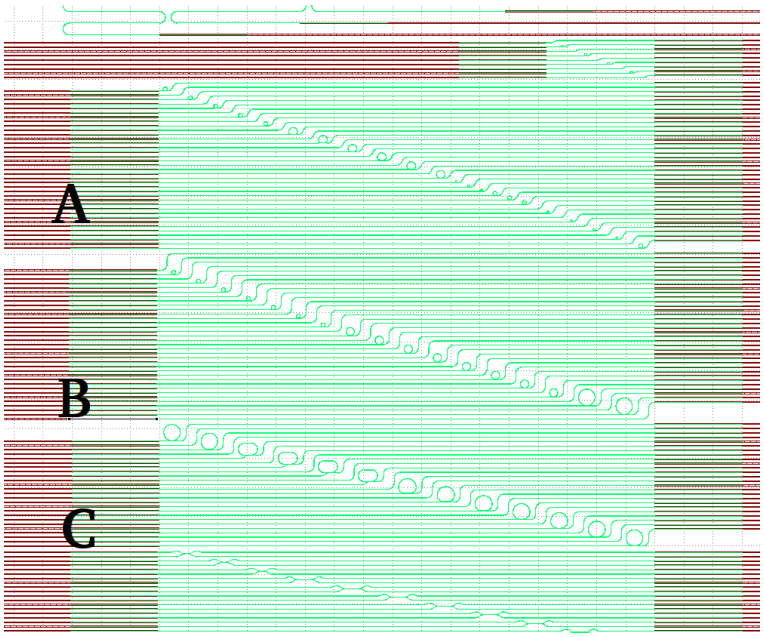

Figure 3.4: Glassgow test structure chip

3.1.2 Toshiba

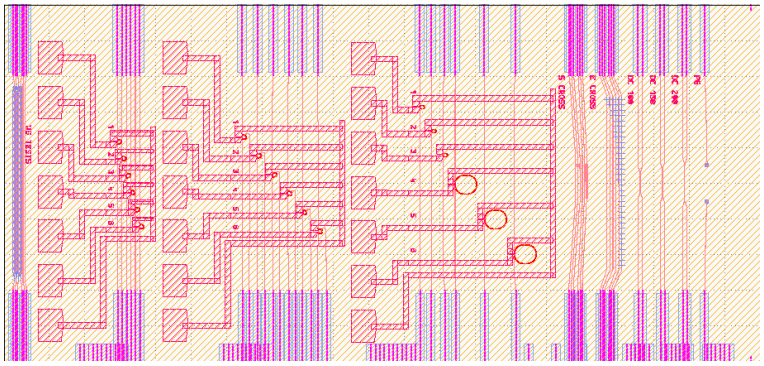

Figure 3.5: Glassgow test structure chip

3.1.3 a-Si

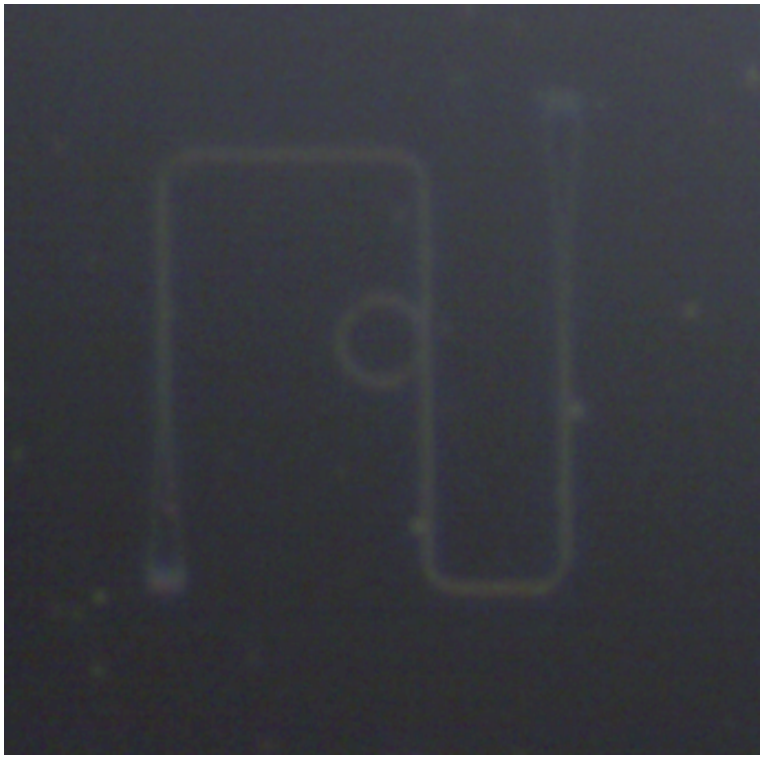

Figure 3.6: Glassgow test structure chip

3.2 Coupling

3.3 Joint Spectrum

Take the convention that the **signal** photon is the one we measure and the **idler** is the one we stimulate.

3.4 What experiments can be done?

Assuming from the above that the procedure for collecting the JSI is fixed and fully understood the question that now needs to be answered is: what parameters can be reliably varied to change the JSI? One that we pursue and that forms the main part of this work is varying the power of the pump laser injected into the ring. This is of interest as it may

3.5 $g^{(2)}(0)$

3.6 Analysing Data

4 Results

4.1 Glassgow

This chip was used to do an initial proof of concept that the JSI of a ring resonator could be measured at high resolution. Here the aim was to explore different ring geometries and develop an intuition on how to do the experiment. The Pritel pulsed laser was used with a pulse duration of 2 ps, a FWHM of 1.0 nm with wavelength range 1530 nm to 1530 nm and a peak power of 100 W. Due to the pulsed laser sometimes destroying the spot size converter on the chip a 3 dB attenuator was added just after the laser output, this resulted in roughly about 5 dB m of power coming out of the lense fiber.

As each device on the chip has unique characteristics due to fabrication errors only some devices produced good data meaning that a full characterisation of the chip was not possible and only a few devices were used. Typically it was imperfections in the spot size converters on the chips being imperfect which prevented good JSI's from being collected but another issue encountered was under coupling of the rings.

Here we present three data sets collected, each has high SNR of at least 20 allowing for the maximum purity P_{max} to be calculated with high accuracy. The relevant spectral scan is presented with the JSIs for reference, these are routine scans performed with the tunable CW laser typically at 1 m W of which roughly -14 dB m gets into the chip.

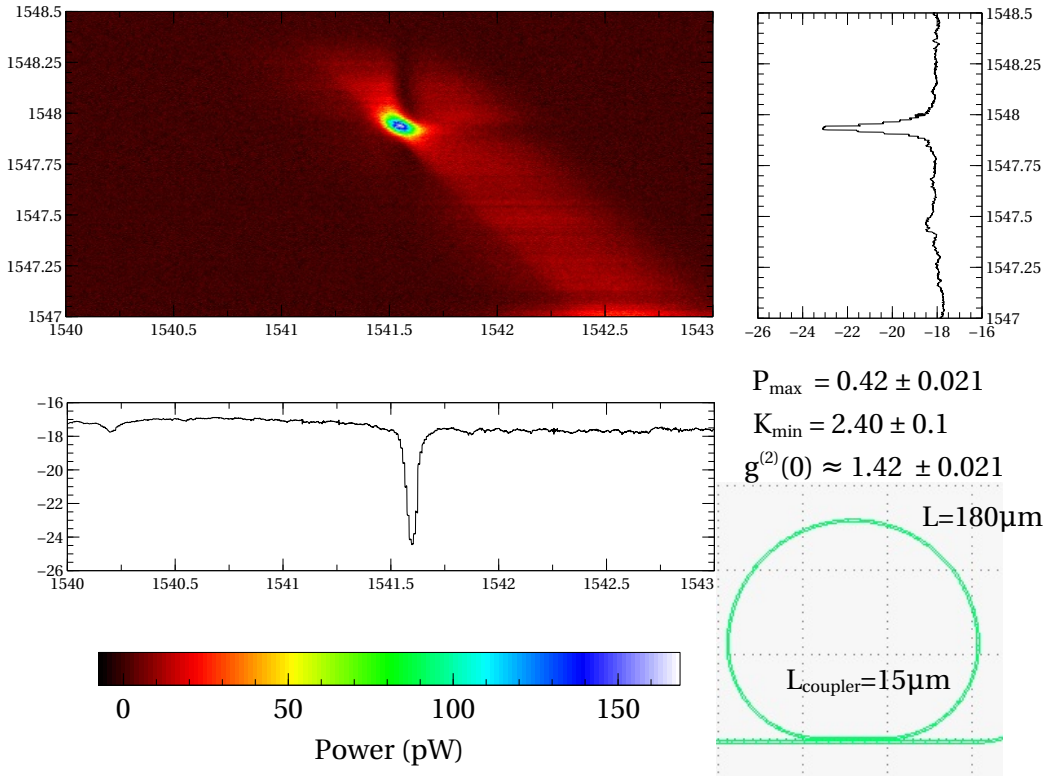

Figure 4.1: JSI Ring C17 We calculate a quality factor of $Q \approx 25000$. In this instance the coupling loss was on average 20 dB and the input power of the pulsed laser was 5.1 dB giving a estimated power in waveguide of -5 dB. The probe laser operated at 1 m W. Fitting the spectral scans of the ring resonators gives coupling parameters of the order $r = 0.946$ $\tau = 0.985$ $n_{eff} = 4.136$, note these are only estimates.

Figure 4.1 shows a clear response from the ring resonator at the resonant frequencies, superimposed on this there is also straight waveguide stimulated four wave mixing observed at much lower intensities. It can be deduced that much of this straight wave guide contribution happens before the ring as it is filtered at the resonance wavelength. The asymmetry is an experimental artefact of imperfect alignment of the resonances with the AWG channels and the pump laser. This is P_{max} value.

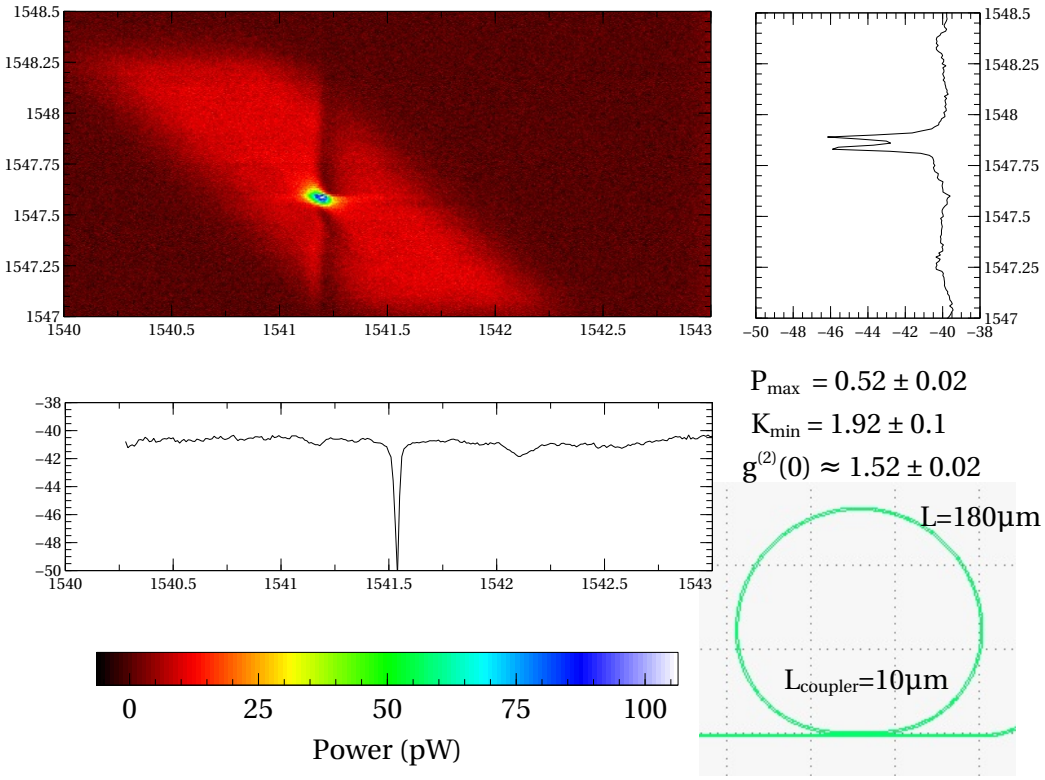

Figure 4.2: JSI Ring C21 We calculate a quality factor of $Q \approx 28000$. In this instance the coupling loss was on average 21 dB and the input power of the pulsed laser was 5.5 dB m giving a estimated power in waveguide of -5 dB m. The probe laser operated at 1 m W. Fitting the spectral scans of the ring resonators gives coupling parameters of the order $r = 0.957$ $\tau = 0.977$ $n_{eff} = 4.144$, note these are only estimates.

In figure 4.2 we see ring C21 which has has many physical similarities with ring C17 shown in figure 4.1 however we observe a few key differences. Firstly the resonance that the CW laser probes is split but this is not reflected in the JSI because the split feature is on the order of 0.01 nm which under the 0.03 nm resolution of the OSA. This inability to resolve finer features which are almost certainly encoded in the real JSA is an important topic discussed later on in this work.

Secondly the coupling distance of the egg shaped resonator is slightly shorter here which is reflected in a slightly smaller value for r, however this difference isn't significant enough to use for a comparison as there are many other factors between the two experiments that were not held

constant, in particular the alignment of the AWG channels.

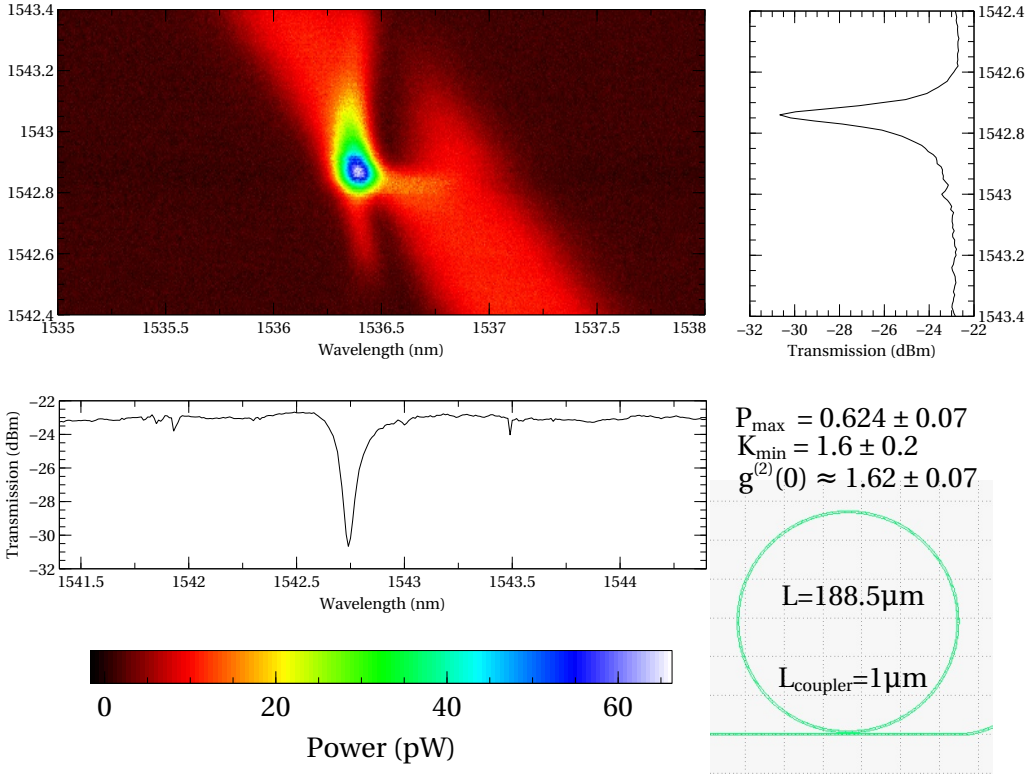

Figure 4.3: JSI Ring B32 We calculate a quality factor of $Q \approx 14000$. In this instance the coupling loss was on average 22 dB m and the input power of the pulsed laser was 5.1 dB m giving a estimated power in waveguide of 0 dB m. The probe laser operated at 1 m W. Fitting the spectral scans of the ring resonators gives coupling parameters of the order $r = 0.985$ $\tau = 0.947$ $n_{eff} = 4.136$, note these are only estimates.

The final JSI collected for this chip is shown in figure 4.3, here the ring geometry is of the more traditional circular shape. It is observed that the resonance has some asymmetry due to more prominent non-linear effects. We observe the intensities of the ring resonator and straight wave guide FWM processes to be more similar in this scan which can be accounted for by the lower quality factory. Again it is notable to see that the ring seems to be collecting some of the straight wave guide FWM, however at a shifted frequency to the peak of the ring FWM, this is contradictory to the two previous examples and may be due to the more non-linear response of this ring.

Summary The three purities observed $(0.42, 0.52, 0.62)$ coincide with previous characterisations of the chip using the single photon detectors which measured a purity of on the order 0.45 [8]. A advantage to these measurements is they allow one to easier develop ways of increasing the purity.

4.2 a-Si

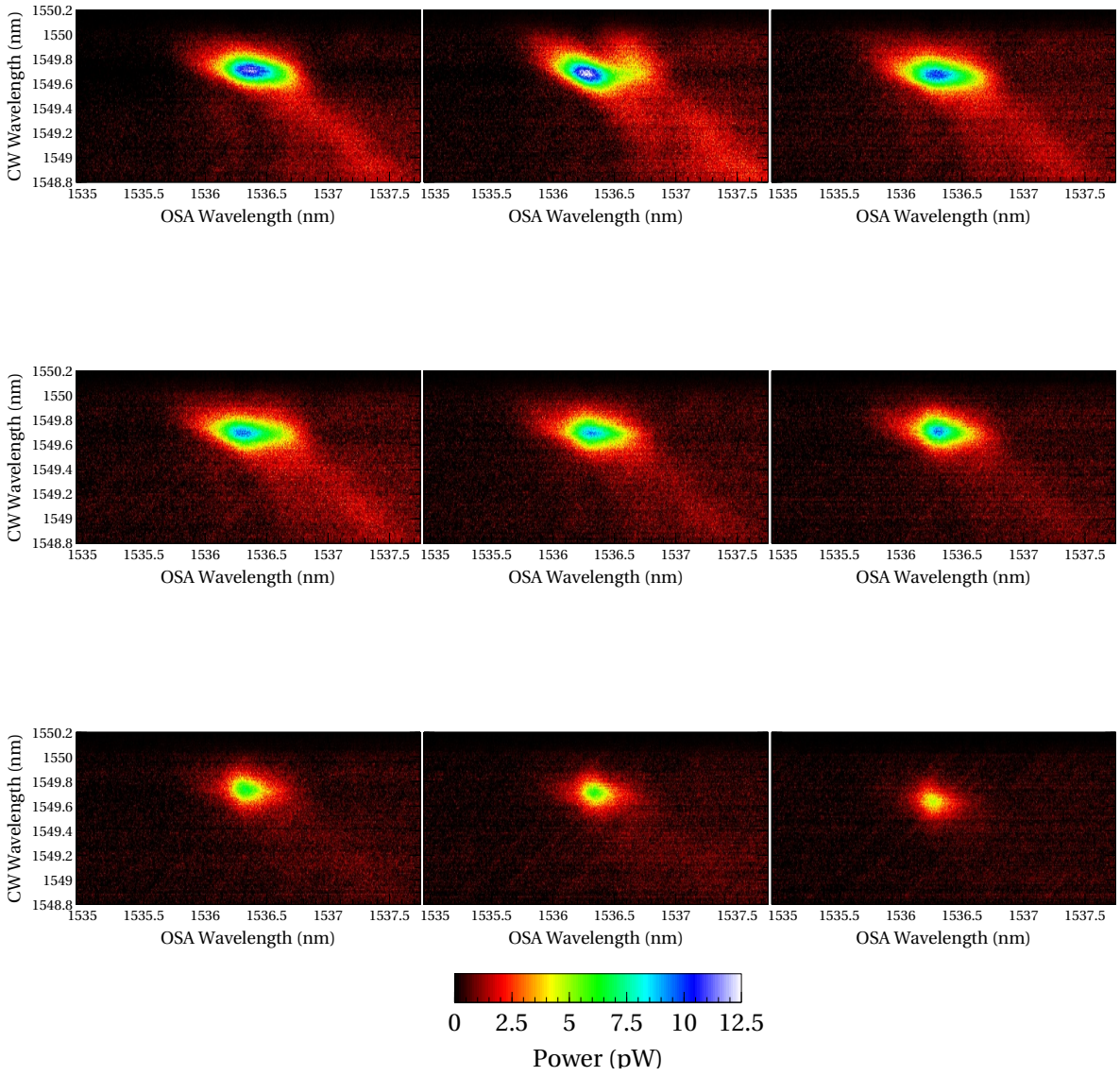

Figure 4.4: tit

4.3 Toshiba

4.3.1 Bistability Data

4.3.2 Pulse shaping

4.3.3 Power Scans

5 Discussion

6 Conclusion

References

[1] E. Knill, R. Laflamme, and G. Milburn. Efficient Linear Optics Quantum Computation. *arXiv:quant-ph/0006088*, June 2000. arXiv: quant-ph/0006088.

[2] David P. DiVincenzo and Daniel Loss. Quantum Information is Physical. *Superlattices and Microstructures*, 23(3-4):419–432, March 1998. arXiv: cond-mat/9710259.

[3] David P. DiVincenzo and IBM. The Physical Implementation of Quantum Computation. *arXiv:quant-ph/0002077*, February 2000. arXiv: quant-ph/0002077.

[4] David C. Burnham and Donald L. Weinberg. Observation of Simultaneity in Parametric Production of Optical Photon Pairs. *Phys. Rev. Lett.*, 25(2):84–87, July 1970.

[5] Vilson R. Almeida and Michal Lipson. Optical bistability on a silicon chip. *Opt. Lett.*, 29(20):2387–2389, October 2004.

[6] Qianfan Xu and Michal Lipson. Carrier-induced optical bistability in silicon ring resonators. *Opt. Lett.*, 31(3):341–343, February 2006.

[7] L. G. Helt, Zhenshan Yang, Marco Liscidini, and J. E. Sipe. Spontaneous four-wave mixing in microring resonators. *Opt. Lett.*, 35(18):3006–3008, September 2010.

[8] Eric Scammell. Indistinguishable Heralded Photons from Silicon Ring Resonators, 2014.

[9] Andreas Eckstein, Guillaume Boucher, Aristide Lematre, Pascal Filloux, Ivan Favero, Giuseppe Leo, John E. Sipe, Marco Liscidini, and Sara Ducci. High-resolution spectral characterization of two photon states via classical measurements. *Laser & Photonics Reviews*, 8(5):L76–L80, September 2014.

A Schmidt Number

A.1 Definition

Starting with some abitrary state ψ:

$$|\psi\rangle = \sum_{i,j} \alpha(i,j)|i\rangle_A \otimes |j\rangle_B \tag{A.1}$$

The schimdt number K of this state measures the degree of entanglement. If $K = 1$ then you can find $|\psi\rangle = |\xi\rangle \otimes |\eta\rangle$ and for $K > 1$ you can find:

$$|\psi\rangle = \sum_{i}^{K} r_i|\xi_i\rangle_A \otimes |\eta_i\rangle_B \tag{A.2}$$

Note that $1 \leq K \leq D$ where D is the dimension of the system. The purity is the inverse of K so:

$$P = 1/K \tag{A.3}$$

An expression for K can be found using the density matrix for ψ:

$$\rho_{AB} = |\psi\rangle\langle\psi| = \sum_{i,j,k,l} \alpha(i,j)\alpha^*(k,l)|i\rangle\langle k| \otimes |j\rangle\langle l| \tag{A.4}$$

$$\rho_A = \mathrm{Tr}_B(\rho_{AB}) = \sum_{i,j,k} \alpha(i,j)\alpha^*(k,j)|i\rangle\langle k| \tag{A.5}$$

$$\rho_A^2 = \sum_{i',j',k'} \sum_{i,j,k} \alpha(i,j)\alpha(k,j)\alpha^*(i',j')\alpha^*(k',j')|i\rangle\langle k|i'\rangle\langle k'| \tag{A.6}$$

$$= \sum_{j',k'} \sum_{i,j,k} \alpha(i,j)\alpha^*(k,j)\alpha(k,j')\alpha^*(k',j')|i\rangle\langle k'| \tag{A.7}$$

$$\mathrm{Tr}_A(\rho_A^2) = \sum_{i,j,k,j'} \alpha(i,j)\alpha^*(k,j)\alpha(k,j')\alpha^*(i,j') \tag{A.8}$$

$$\tag{A.9}$$

For a unentangled ψ we know that $\mathrm{Tr}_A(\rho_A^2) = 1$ For ψ entangled this will be smaller than 1 (proof comes from the property of the density operator that its eigenvalues are all smaller than 1). This fits the definiton of the purity of a quantum state hence we can write:

$$P = \frac{1}{K} = \sum_{i,j,k,l} \alpha(i,j)\alpha^*(k,j)\alpha(k,l)\alpha^*(i,l) \tag{A.10}$$

A.2 Calculation from experimental data

A.2.1 Trace method

In the lab we can measure $|\phi(\omega_1, \omega_2)|^2$, here I outline how to extract the schimdt number from this set of values. Taking the positive square root of the matrix of values obtained from the lab you have a matrix $\mathbf{f}$ given by:

$$\mathbf{f} = \sum_{\omega_1,\omega_2} \phi(\omega_1,\omega_2)|\omega_1\rangle\langle\omega_2| \tag{A.11}$$

(This seems to be some weird way of writing the wavefunction as a matrix, bare with me it turns out to be useful)

$$\mathbf{f}^\dagger\mathbf{f} = \sum_{\omega_1,\omega_2,\omega_3} \phi(\omega_1,\omega_2)\phi(\omega_3,\omega_2)|\omega_1\rangle\langle\omega_3| \tag{A.12}$$

$$(\mathbf{f}^\dagger\mathbf{f})^2 = \sum_{\omega_1,\omega_2,\omega_3,\omega_4,\omega_5,\omega_6} \phi(\omega_1,\omega_2)\phi(\omega_3,\omega_2)\phi(\omega_4,\omega_5)\phi(\omega_6,\omega_5)|\omega_1\rangle\langle\omega_3|\omega_4\rangle\langle\omega_6| \tag{A.13}$$

$$(\mathbf{f}^\dagger\mathbf{f})^2 = \sum_{\omega_1,\omega_2,\omega_3,\omega_4,\omega_5,\omega_6} \phi(\omega_1,\omega_2)\phi(\omega_3,\omega_2)\phi(\omega_3,\omega_5)\phi(\omega_6,\omega_5)|\omega_1\rangle\langle\omega_6| \tag{A.14}$$

$$\mathrm{Tr}\left[(\mathbf{f}^\dagger\mathbf{f})^2\right] = \sum_{\omega_1,\omega_2,\omega_3,\omega_4} \phi(\omega_1,\omega_2)\phi(\omega_3,\omega_2)\phi(\omega_3,\omega_4)\phi(\omega_1,\omega_4) \tag{A.15}$$

I've done it this way because I wanted to figure out where the equation in [9] comes from. You can now see that equation A.10 is of exactly the same form as $\mathrm{Tr}\left[(\mathbf{f}^\dagger\mathbf{f})^2\right]$ (barring the conjugates but this is okay since ϕ is real.) Taking the parallel further it can be seen that equation A.12 is of the form of a reduced density matrix. Here we must make sure to normalise to make sure this is a valid reduced density matrix. The normalisation is:

$$N = \mathrm{Tr}\left[\mathbf{f}^\dagger\mathbf{f}\right] = \sum_{\omega_1,\omega_2} \phi(\omega_1,\omega_2)^2 \tag{A.16}$$

Giving:

$$\rho_A = \frac{\mathbf{f}^\dagger\mathbf{f}}{N} \tag{A.17}$$

We can then write:

$$\frac{1}{K} = \frac{\mathrm{Tr}\left[(\mathbf{f}^\dagger\mathbf{f})^2\right]}{\mathrm{Tr}\left[\mathbf{f}^\dagger\mathbf{f}\right]^2} \tag{A.18}$$

B Equipment Specifications

C Transfer matrix analysis of ring resonator cavities

A useful way to describe the spectral response of a ring resonator is by defining a transfer matrix. This 2×2 matrix relates the electric fields of the inputs and outputs of the waveguide and resonator. In our analysis we define the electric fields to be complex valued and also normalised to conserve energy, this condition implies the transfer matrix must be unitary.

First write down the obvious relations

$$E_{out} = r_1 E_{in} + t_1 E_2 \tag{C.1}$$

$$E_1 = r_2 E_2 + t_2 E_{in} \tag{C.2}$$

Define a matrix.

$$M = \begin{pmatrix} r_1 & t_1 \\ t_2 & r_2 \end{pmatrix} \tag{C.3}$$

Enforce unitarity

$$\begin{pmatrix} r_1 & t_1 \\ t_2 & r_2 \end{pmatrix} \begin{pmatrix} r_1^* & t_2^* \\ t_1^* & r_2^* \end{pmatrix} = \begin{pmatrix} |r_1|^2 + |t_1|^2 & r_1 t_2^* + r_2^* t_1 \\ r_2 t_1^* + r_1^* t_2 & |r_2|^2 + |t_2|^2 \end{pmatrix} = \begin{pmatrix} 1 & 0 \\ 0 & 1 \end{pmatrix} \tag{C.4}$$

Furthermore $\det M = 1$

$$r_1 r_2 - t_1 t_2 = 1 \tag{C.5}$$

so

$$r_2 = \frac{1 + t_1 t_2}{r_1} \tag{C.6}$$

Also $M^{-1} = M^*$

$$\begin{pmatrix} r_2 & -t_1 \\ -t_2 & r_1 \end{pmatrix} = \begin{pmatrix} r_1^* & t_1^* \\ t_2^* & r_2^* \end{pmatrix} \tag{C.7}$$

This tells us r_1 and r_2 must be real. So we can simplify the unitarity equation. So

$$t_1 = iT_1 \tag{C.8}$$

$$t_2 = iT_2 \tag{C.9}$$

Rewrite the interesting equations: Use also $r_2 = r_1^*$

$$\begin{pmatrix} |r_1|^2 + T_1^2 & -ir_1 T_2 + ir_1 T_1 \\ -ir_1^* T_1 + ir_1^* T_2 & |r_1|^2 + T_2^2 \end{pmatrix} = \begin{pmatrix} 1 & 0 \\ 0 & 1 \end{pmatrix} \tag{C.10}$$

Ok so $T_2 = T_1 = t$

$$\begin{pmatrix} |r_1|^2 + t^2 & 0 \\ 0 & |r_1|^2 + t^2 \end{pmatrix} = \begin{pmatrix} 1 & 0 \\ 0 & 1 \end{pmatrix} \tag{C.11}$$

$$|r_1|^2 = 1 - t^2 \tag{C.12}$$

$$|r_2|^2 = 1 - t^2 \tag{C.13}$$

d Basically I have a degree of freedom. $r_1 = e^{i\theta}r$ and $r_2 = e^{-i\theta}r$. Choose $\theta = 0$ for simplicity.

Now the matrix is:

$$\begin{pmatrix} r & it \\ it & r \end{pmatrix} \tag{C.14}$$

Now we add that

$$E_2 = \tau e^{i\theta} E_1$$

Recall the initial equations.

$$E_{out} = rE_{in} + itE_2 \tag{C.15}$$

$$E_1 = rE_2 + itE_{in} \tag{C.16}$$

$$E_1 = r\tau e^{i\theta} E_1 + itE_{in} \tag{C.17}$$

$$\frac{E_1}{E_0} = \frac{it}{1 - r\tau e^{i\theta}} \tag{C.18}$$

Okay so thats E_1 done.

$$\frac{E_1}{E_0} = \frac{it}{1 - r\tau e^{i\theta}} \tag{C.19}$$

$$\left|\frac{E_1}{E_0}\right|^2 = \frac{t^2}{1 + r^2\tau^2 - 2r\tau cos(\theta)} \tag{C.20}$$

For E_2 we have:

$$\frac{E_2}{E_0} = \frac{it\tau e^{i\theta}}{1 - r\tau e^{i\theta}} \tag{C.21}$$

$$\left|\frac{E_2}{E_0}\right|^2 = \frac{\tau^2 - \tau^2 r^2}{1 + r^2\tau^2 - 2r\tau cos(\theta)} \tag{C.22}$$

For E_{out} we have:

$$\frac{E_{out}}{E_0} = r + it\frac{it\tau e^{i\theta}}{1 - r\tau e^{i\theta}} \tag{C.23}$$

$$\frac{E_{out}}{E_0} = \frac{r - r^2\tau e^{i\theta} - t^2\tau e^{i\theta}}{1 - r\tau e^{i\theta}} \tag{C.24}$$

$$\left|\frac{E_{out}}{E_0}\right|^2 = \frac{(r - r^2\tau e^{i\theta} - t^2\tau e^{i\theta})(r - r^2\tau e^{-i\theta} - t^2\tau e^{-i\theta})}{(1 - r\tau e^{i\theta})(1 - r\tau e^{-i\theta})} \tag{C.25}$$

$$\left|\frac{E_{out}}{E_0}\right|^2 = \frac{(r(r - r^2\tau e^{-i\theta} - t^2\tau e^{-i\theta}) - r^2\tau e^{i\theta}(r - r^2\tau e^{-i\theta} - t^2\tau e^{-i\theta}) - t^2\tau e^{i\theta}(r - r^2\tau e^{-i\theta} - t^2\tau e^{-i\theta}))}{1 + r^2\tau^2 - 2r\tau cos(\theta)} \tag{C.26}$$

$$\left|\frac{E_{out}}{E_0}\right|^2 = \frac{r^2 - r^3\tau e^{-i\theta} - rt^2\tau e^{-i\theta} - r^3\tau e^{i\theta} + r^4\tau^2 + 2r^2\tau^2 t^2 - rt^2\tau e^{i\theta} + t^4\tau^2}{1 + r^2\tau^2 - 2r\tau cos(\theta)} \tag{C.27}$$

$$\left|\frac{E_{out}}{E_0}\right|^2 = \frac{r^2 - e^{-i\theta}(r^3\tau + rt^2\tau) - e^{i\theta}(r^3\tau + rt^2\tau) + r^4\tau^2 + t^4\tau^2 + 2r^2\tau^2 t^2}{1 + r^2\tau^2 - 2r\tau cos(\theta)} \tag{C.28}$$

$$\left|\frac{E_{out}}{E_0}\right|^2 = \frac{r^2 + 2(r^3\tau + rt^2\tau)\cos(\theta) + r^4\tau^2 + t^4\tau^2 + 2r^2\tau^2 t^2}{1 + r^2\tau^2 - 2r\tau cos(\theta)} \tag{C.29}$$

$$\left|\frac{E_{out}}{E_0}\right|^2 = \frac{r^2 2(r^3\tau + r(1-r^2)\tau)\cos(\theta) + r^4\tau^2 + (1-r^2)^2\tau^2 + 2r^2\tau^2(1-r^2)}{1 + r^2\tau^2 - 2r\tau cos(\theta)} \tag{C.30}$$

$$\left|\frac{E_{out}}{E_0}\right|^2 = \frac{r^2 - 2(r^3\tau + r(1-r^2)\tau)\cos(\theta) + r^4\tau^2 + (1-2r^2+r^4)\tau^2 + 2r^2\tau^2 - 2r^4\tau^2}{1 + r^2\tau^2 - 2r\tau cos(\theta)} \tag{C.31}$$

$$\left|\frac{E_{out}}{E_0}\right|^2 = \frac{r^2 - 2r\tau\cos(\theta) + r^4\tau^2 + \tau^2 - 2r^2\tau^2 + r^4\tau^2 + 2r^2\tau^2 - 2r^4\tau^2}{1 + r^2\tau^2 - 2r\tau cos(\theta)} \tag{C.32}$$

FINAL RESULTS

$$\left|\frac{E_{out}}{E_0}\right|^2 = \frac{r^2 - 2r\tau\cos(\theta) + \tau^2}{1 + r^2\tau^2 - 2r\tau cos(\theta)} \tag{C.33}$$

$$\left|\frac{E_2}{E_0}\right|^2 = \frac{\tau^2 - \tau^2 r^2}{1 + r^2\tau^2 - 2r\tau cos(\theta)} = \tau^2\left|\frac{E_1}{E_0}\right|^2 \tag{C.34}$$

$$\left|\frac{E_1}{E_0}\right|^2 = \frac{t^2}{1 + r^2\tau^2 - 2r\tau cos(\theta)} \tag{C.35}$$